Chemical Engineering Journal 523 (2025) 168357

Contents lists available at ScienceDirect

Chemical Engineering Journal

journal homepage: www.elsevier.com/locate/cej

Covalent organic frameworks (COFs) functionalized with boronate and triazole moieties for selective adsorption of D-fructose

Tobias Riedl [a], Pia Groß [a], Leonie Sophie Häser [a], Runa Tschekorsky Orloff [a], Theresa Röper [a], Thomas Fuchs [b], Stephanie Bachmann [c], Ann-Christin Pöppler [c], Herwig Peterlik [d], Andreas Jupke [b], Regina Palkovits [a,e,f], Irina Delidovich [g,*]

[a] Chair of Heterogeneous Catalysis and Chemical Technology, RWTH Aachen University, Worringerweg 2, 52074, Aachen, Germany
[b] Fluid Process Engineering (AVT.FVT), RWTH Aachen University, Forckenbeckstraße 51, 52074, Aachen, Germany
[c] Institute of Organic Chemistry, University of Würzburg, Am Hubland, 97074, Würzburg, Germany
[d] Faculty of Physics, University of Vienna, Boltzmanngasse 5, 1090, Vienna, Austria
[e] Institute for a Sustainable Hydrogen Economy, Forschungszentrum Jülich, Marie-Curie-Str. 5, 52428, Jülich, Germany
[f] Max Planck Institute for Chemical Energy Conversion, Stiftstraße 34–36, 45470, Mülheim an der Ruhr, Germany
[g] Institute of Chemical, Environmental and Bioscience Engineering, TU Wien, Getreidemarkt 9, 1060, Vienna, Austria

ARTICLE INFO

Keywords:
Covalent organic frameworks
Adsorption
Fructose
Boronate
Triazole

ABSTRACT

Development of efficient downstream processes presents one of the central issues in biorefining. In this respect, synthesis of tailored adsorbents for separation of saccharides from product streams is a major challenge. In this study, separation of D-fructose and D-glucose over covalent organic frameworks functionalized with boronate moieties is proposed. Two-dimensional COFs were synthesized *via* condensation of a tripodal amine linker with dipodal aldehyde linkers to obtain scaffolds bearing propargyl moieties, which were post-synthetically modified *via* an azide click reaction. The materials obtained were characterized by N_2 physisorption, ^{1}H, ^{13}C and ^{11}B MAS NMR spectroscopy, SAXS, FTIR spectroscopy, and SEM. The COFs functionalized with boronate moieties exhibit outstanding Langmuir D-fructose adsorption capacity up to 560 mg g^{-1}. D-fructose can be efficiently desorbed by washing with sulfuric acid solution, and the adsorbent can be recycled four times. Adsorption tests over COFs bearing different functionalities suggest formation of covalent bonds with boronates as well as non-covalent interactions with triazole moieties as driving forces of the adsorption of D-fructose and D-glucose. The results of adsorption under batch and continuous conditions evidence the high potential of the synthesized COFs for adsorptive separation of D-glucose and D-fructose.

1. Introduction

Dependence of the chemical industry on oil, natural gas, and coal has been a matter of concern for decades and attempts to move from exhaustible fossil resources to renewable raw materials have been undertaken. Numerous factors encourage transition from oil to biomass, including climate changes as well as global and national energy security [1]. Valorization of cellulose readily available as part of agricultural wastes *via* novel platform molecules presents a promising approach [2–13]. In this regard, 5-(hydroxymethyl)furfural (HMF) is a platform chemical with a strong potential as an intermediate for production of renewable polymers, fuel additives, as well as other commodities and fine chemicals [14,15]. Modest yields were reported for transformation of D-glucose into HMF, while higher performances were achieved for synthesis of HMF based on D-fructose. R&D activity of Avantium company resulted in a method for production of furanics *via* dehydration of D-fructose in methanol as solvent with a claimed yield of HMF of 70 % [16].

Nowadays, D-fructose is manufactured as a component of high fructose corn syrup (HFCS; 42–55 % D-fructose, rest D-glucose, and 1–4 % oligosaccharides), a liquid alternative sweetener made from corn starch. Isomerization of D-glucose into D-fructose is catalyzed by immobilized glucose isomerase (GI, EC 5.3.1.5; also known as D-xylose isomerase XI). This is by far the largest synthetic biocatalytic process [17]. The major applications of HFCS are now carbonated beverages and raised bakery products. Due to thermodynamic and kinetic limitations, manufacturing

* Corresponding author.
E-mail address: irina.delidovich@tuwien.ac.at (I. Delidovich).

https://doi.org/10.1016/j.cej.2025.168357
Received 17 July 2025; Received in revised form 8 September 2025; Accepted 10 September 2025
Available online 12 September 2025

plants typically settle for the yield of D-fructose below 42 % [18].

Chromatographic separation of D-glucose and D-fructose after isomerization is one of the largest separations of biomass-based products developed in the 1970^s [19]. Gel-type, slightly cross-linked cation exchange resins in Ca^{2+} form are used as stationary phases for the chromatography [20]. Noteworthily, moderate separation factors of D-glucose and D-fructose in the range of 1.5–3.5 present a serious disadvantage of Ca^{2+} ion exchange resins [19,21,22]. Development of novel adsorbents, which would enable highly selective separation of D-glucose and D-fructose, is a long-standing scientific question that remains nowadays interesting and timely.

Adsorbents capable of highly selective separation of D-glucose and D-fructose with separation factors of 10–20 were reported in the 1970^s [23,24]. These are materials functionalized with boronic acid groups which can be ionized into boronate groups. The latter can reversibly complex saccharides yielding complexes of various stability (complexations constants are $K_{compl.} = 65$ for D-glucose and $K_{compl.} = 1698$ for D-fructose [25]), thus enabling chromatographic separation of these saccharides. Using alkaline eluents at pH 8.3–10.5 gives rise to narrow peaks with excellent separation [23,24,26]. Application of a fixed-bed adsorber to selectively adsorb D-fructose from its mixture with D-glucose under alkaline conditions and recovery of D-fructose upon washing with an acidic solution presents an alternative to chromatographic separation (Fig. S1) [27]. A rational design of an absorbent meeting the requirements – such as large adsorption capacity and high selectivity for D-fructose uptake, recyclability, along with chemical and mechanical stability under working conditions – poses a challenge. Gel-type cross-linked polymers exhibit high binding capacity of D-fructose of up to 540 $mg_{D\text{-}fructose}/g_{polymer}$ but suffer from slow kinetics of uptake and low mechanical stability owing to a swelling degree of up to 212 % [25,28–30]. Recently, macroporous boron-containing materials were proposed for adsorption of saccharides [31–37]. These adsorbents exhibit low swelling degree and improved kinetics of uptake but manifest lower loadings of sugars (54 mg g^{-1} D-tagatose, an isomer of D-fructose) due to not fully accessible boronate adsorption sites. Grafting of boronate groups onto a tailor-made support enables quick and full access to all the boronate groups [38–42] though with low binding capacities (*e.g.* 14 $mg_{D\text{-}fructose}/g_{polymer}$ [42]) due to low boron content. Grafting of polymer chains functionalized with boronates presents a recently proposed synthetic approach, which enables up to 381 $mg_{D\text{-}glucose}/g_{polymer}$ loading of D-glucose onto grafted polymer brushes on SBA-15 [43]. In summary, a support matrix presents a major challenge for a rational design of a material bearing phenylboronate groups [44]. Organic polymeric matrices suffer from swelling, low accessibility of phenylboronic groups owing to high cross-linking degree, and low water-wettability due to the hydrophobic nature of the polymers. Inorganic – such as silica – or organic-inorganic hybrid support matrices were proposed to mitigate these problems. Unfortunately, these materials exhibit poor stability in alkaline or acidic media, *i.e.* under adsorption and desorption conditions [44].

Covalent organic frameworks (COFs) are a young class of crystalline porous polymers [45] whose backbone is composed exclusively of light elements – carbon, oxygen, nitrogen, silicium, or boron – connected by covalent bonds. COFs are potentially excellent adsorbents owing to their large specific surface areas, low densities, monomodal size distributions of nanopores, readily adjustable pore sizes and chemical environment, and regular porosities [46]. Few examples of functionalization of COF backbone with boronate groups as adsorption sites were reported: for instance, for specific enrichment of glycopeptides [47,48], monoamine neurotransmitters [49], 1,2-dihydroxyanthracene-9,10-dione [50], and hydrophilic nucleosides [51] along with uranium extraction and I_2 capture [52]. To our knowledge, boronate-functionalized COFs have not been reported for recovery of saccharides in biorefining yet.

In this work, two-dimensional COFs bearing propargyl groups were synthesized and post-synthetically functionalized with boronate groups using an azide click reaction. The obtained materials exhibit high maximum Langmuir adsorption capacity of D-fructose up to 560 mg g^{-1}, excellent selectivity for D-fructose uptake, recyclability, and high robustness owing to no swelling during adsorption.

2. Experimental

2.1. Chemicals

Unless specified, all chemicals were used without further purification. Dichloromethane (DCM, ≥ 98 %), 1,2-dichlorobenzene (≥98 %), 1-butanol (>99.9 %), and dimethylsulfoxide (99.7 %) were purchased at Sigma Aldrich. Tetrahydrofuran (THF, >99.5 %), toluene (>99.5 %), ethanol (EtOH, >99.9 %), acetone (>99.5 %), hydrochloric acid (37 wt %), sulfuric acid (>99 %), and acetic acid (>99.5 %) were supplied by Chemsolute. The bases diethanolamine (99 %), N,N-diisopropylethylamine (DIPEA, >99 %), potassium carbonate (>99 %), sodium hydroxide (>99.5 %) as well as the buffer solutions of glycine (pH 12, 99 %) and potassium hydrogenphosphate (pH 8, 99 %) were purchased from Roth. The monomer building blocks 1,3,5-tribromobenzene (>99 %), 4-aminophenyl boronic acid pinacol ester (>98 %), 2,5-dimethoxybenzene-1,4-dicarboxaldehyde (>99 %), 4-(azidomethyl)benzeneboronic acid pinacol ester (>99 %) as well as the propargylation reagent propargyl bromide (80 % in toluene) were provided by TCI chemicals. The demethylation reagent boron tribromide solution (1.0 M) in dichloromethane, the two catalysts copper (I) bromide (>98.5 %) and tetrakis(triphenylphosphine)palladium (0) (99 %) were supplied by Alfa Aesar. D-(−)-Fructose (>99.5 %) and D-(+)-glucose (>99.5 %) were purchased from Roth. The labeled sugars ^{13}C-2-D-fructose (99 %) and ^{13}C-1-D-glucose (99 %) were purchased from Euriso-Top.

2.2. Synthesis of monomers and COFs

Methoxy-COF was obtained *via* polymerization of DMTA with TAPB in the presence of acetic acid at 120 °C for 72 h. $(HC{\equiv}C)_{0.5}$-COF and $(HC{\equiv}C)_{1.0}$-COF were prepared *via* polymerization of respective amounts of DMTA, BPTA, and TAPB. Protected $(P\text{-}B)_{0.5}$-COF and $(P\text{-}B)_{1.0}$-COF were synthesized *via* post synthetic modification of $(HC{\equiv}C)_{0.5}$-COF and $(HC{\equiv}C)_{1.0}$-COF with 4(azidomethyl)benzeneboronic acid pinacol ester. The deprotection of $(P\text{-}B)_{0.5}$-COF and $(P\text{-}B)_{1.0}$-COF was performed by hydrolysis in HCl solution. Triazole-COF was obtained by the reaction of $(HC{\equiv}C)_{0.5}$-COF with benzyl azide. Details of syntheses of the monomers and the COFs are provided in electronic supplementary information (ESI).

2.3. Characterization of materials

The nitrogen adsorption isotherms were recorded at 77 K using a Micromeritics ASAP 2060. Before each measurement, the samples were degassed at 150 °C under vacuum for at least 5 h using a FloVac. FTIR spectra were recorded with a Fourier Transform Infrared Spectrometer from Jasco (FT/IR-4600) with a resolution of 4 cm^{-1} in the wavelength range from 4000 to 500 cm^{-1} with the related software Spectra Manager Version 2.13.00. Elemental analysis was performed using an ICP-OES Spectroblue Instrument from Spectro Analytical Instruments. Prior to the measurements, 30 mg sample were digested in a solution of HF (800 mL water, 160 mL HF and 40 mL H_2SO_4) by holding it for 30 min in a microwave oven (600 W, 120 °C). The scanning electron microscope images were taken using a COXEM EM-30AX. The high voltages were used in a variable range of 5–15 kV. The samples were coated with Au before measurement using a COXEM sputter at 9 mA for 200 s. Solution NMR spectroscopy was conducted using a Bruker AV III 400 MHz instrument at room temperature.

Solid-state NMR investigations of the COFs were performed on a Bruker Avance III HD 600 MHz NMR spectrometer at 20 kHz MAS using a 3.2 mm HX probe. For ^{1}H–^{13}C cross-polarization (CP) experiments, a 2

ms contact time with a ramp on the ^{1}H channel and an interscan delay of 1 s were used. ^{13}C NMR experiments with direct excitation (DE) and a short interscan delay of 2 s were measured to probe mobility. During acquisition of ^{13}C NMR spectra, SPINAL64 heteronuclear decoupling was employed. ^{11}B NMR spectra were acquired using the Hahn echo sequence to reduce the background signal from the probe. Chemical shifts were referenced using adamantane setting the left signal to 38.48 ppm by adjusting the field value of the spectrometer according to IUPAC recommendations [53]. As the signal intensity of D-fructose and D-glucose was too low at natural abundance to quantify the amount of respective species, a second batch of samples with labeled ^{13}C-2-D-fructose and ^{13}C-1-D-glucose was produced and measured. Here, for ^{13}C CP MAS spectra an interscan delay of 2 s was used, ^{13}C DE spectra were recorded with 2 s and 20 s interscan delays. Samples with the labeled sugars were measured at 273 K, whereas all other samples were measured at room temperature. Frictional heating due to MAS results in a higher actual sample temperature (≈+30 K at 20 kHz MAS). Spectral processing was done using the Bruker TopSpin 4.0.8 software.

For small-angle X-ray scattering (SAXS) analysis, samples were placed between two tapes in a holder and measured for 900 s in vacuum in a Bruker AXS Nanostar with a pinhole collimated beam and CuKα radiation generated by a microfocus source. Scattering patterns were recorded with a 2D area detector (VANTEC 2000). Data were radially integrated, normalized by the transmission obtained from a transparent beamstop and background subtracted. SAXS intensities are shown in dependence on the scattering vector $q = (4\pi/\lambda)\sin(\theta)$ with 2θ being the scattering angle and $\lambda = 0.1542$ nm the X-ray wavelength. The COF samples after adsorption and desorption were separated by filtration and dried under vacuum at room temperature prior to examination by SAXS.

2.4. Sorption performance

2.4.1. Adsorption in batch

The carbonate buffer solution was obtained by dissolution of 7 g $NaHCO_3$ in 100 mL water and adjustment of the obtained solution to pH 10 by a dropwise addition of 4 M NaOH. The phosphate buffer solutions were prepared by dissolution of 2.08 g KH_2PO_4 in 30 mL water and a dropwise addition of 4 M NaOH to obtain pH 7.5 or 8, respectively. To prepare the acetate buffer, 3.03 g CH_3COONa were dissolved in 30 mL water and 1 M CH_3COOH was dropwise added to this solution to adjust pH to 5.

For each experiment, a blind sample without COF was measured. The solutions for recording adsorption isotherms were prepared by dissolving 75–750 mg of either D-glucose or D-fructose in 3 mL carbonate buffer solution. Each solution (1.5 mL) was added to 35–40 mg COF and the resulting suspension was stirred at 500 rpm at room temperature (RT). The solutions were filtered with polyamide syringe filters (Chromafil PA 20/25) and diluted *via* addition of 0.5 mL filtered solution to 2 mL water. The obtained solution was stirred with 50 mg Amberlyst©15 in H^+ form for 15 min at RT. The solution was decanted and stirred with Amberlyte©IR-96 for 30 min at RT. The obtained after decantation solution was analysed by HPLC.

To study a competitive adsorption, a 1:1 mixture was prepared *via* dissolution of 75 mg D-glucose and 75 mg D-fructose in 3 mL carbonate buffer at pH 10. A 1:4 mixture was obtained *via* dissolution of 30 mg D-fructose and 120 mg D-glucose in 3 mL carbonate buffer at pH 10. Competitive adsorption experiments were conducted *via* stirring 1.5 mL a mixture of D-glucose and D-fructose in carbonate buffer with 40 mg COF at RT.

2.4.2. Desorption and recycling

150 mg D-fructose were dissolved in 3 mL carbonate buffer at pH 10. 1.5 mL of the obtained solution were stirred with 40 mg $B_{0.5}$-COF for 3 h at RT. Thereafter the suspension was filtered on a glass frit. The loaded COF was stirred in 1.5 mL of desorption solution for 3 h at RT. The solutions were filtered with polyamide syringe filters (Chromafil PA 20/25) and diluted *via* addition of 0.5 mL filtered solution to 2 mL water. The obtained solution was stirred with 50 mg Amberlyst©15 in H^+ form for 15 min at RT. The solution was decanted and stirred with Amberlyte©IR-96 for 30 min at RT. The obtained after decantation solution was analysed by HPLC.

In the recycling study, four adsorption and desorption cycles were conducted. The $B_{0.5}$-COF was filtered on a por. 4 filter crucible and used in the next adsorption or desorption cycle without drying.

2.4.3. Column experiments

Column pulse experiments were conducted using a mixture of D-fructose with D-glucose. A defined amount of the mixture was introduced into the system *via* an injection loop. The eluent flow was started, and the sugar mixture was injected into the system, passing through a pressure-resistant glass column (VDS OptiLab, 7 mL) packed with 700 mg of $B_{0.5}$-COF. A solution with a glucose-to-fructose ratio of 1:1 and a total sugar concentration of 50 mg mL^{-1} was used. The volumetric flow rate was set to 0.5 mL min^{-1}, and a pulse duration was 10 min. After elution through the column, the mixture was analysed using a UV spectrometer and a refractometer. The eluent flow was fractionated, and the sugar content in each fraction was determined using high-performance liquid chromatography (HPLC). A scheme of the used setup is provided in ESI.

3. Results and discussion

3.1. Synthesis and characterization of COFs

Two-dimensional COFs with imine bonds were synthesized based on the monomers 2,5-bis(prop-2-yn-1-yloxy)terephthalaldehyde (BPTA), 1,3,5-tris(4-aminophenyl)benzene (TAPB), and 2,5-dimethoxyterephthalaldehyde (DMTA) as schematically shown in Fig. 1. BPTA monomer was synthesized *via* demethylation of commercially available DMTA with boron tribromide followed by propargylation. TAPB was prepared from 1,3,5-tribromobenzene *via* a palladium catalyzed cross-coupling. NMR spectra of the used monomers are provided in ESI (Figs. S2 and S3).

The TAPB tripodal amine linker and the BPTA and DMTA dipodal aldehyde linkers were used in a Schiff-base polymerization performed using CH_3COOH as a catalyst following a somewhat modified previously reported procedure [54]. At the end of the syntheses, no signals of the monomers in ^{1}H NMR spectra in solution were observed suggesting their complete incorporation into the solid products. The obtained materials were characterized by low-temperature N_2 physisorption (Fig. 2), FTIR spectroscopy, solid-state ^{1}H, ^{13}C, and ^{11}B NMR spectroscopy, and SEM. Crystalline structure of the obtained COFs was explored by means of SAXS. The boron content was determined by ICP-OES.

Condensation of TAPB and DMTA gave rise to Methoxy-COF polymer. The obtained material exhibited a specific surface area of 792 $m^2\ g^{-1}$, an external specific surface area of 430 $m^2\ g^{-1}$, and a total pore volume of 0.525 $cm^3\ g^{-1}$. The ^{13}C MAS NMR spectrum of Methoxy-COF (Fig. 3) exhibits characteristic resonances of TAPB in the range of 115 to 155 ppm along with the signals of the aromatic carbon atoms and ether groups of DMTA at 108 and 55 ppm, respectively.

Co-polymerization of TAPB and BPTA resulted in $(HC{\equiv}C)_{1.0}$-COF, whereas a mixture of TAPB, BPTA, and DMTA using an equivalent ratio of the aldehyde monomers led to $(HC{\equiv}C)_{0.5}$-COF. A characteristic band at 3300 cm^{-1} corresponding to a CH function on a C≡C triple bond was observed in the FTIR spectra (Fig. S4). Moreover, resonances at 70 and 80 ppm of the C≡C group were present in ^{13}C solid-state NMR spectra (Fig. 3). The $(HC{\equiv}C)_{1.0}$-COF and $(HC{\equiv}C)_{0.5}$-COF exhibited specific surface areas of 278 $m^2\ g^{-1}$ and 590 $m^2\ g^{-1}$, respectively. Low-pressure high-resolution N_2 physisorption revealed a microporous structure with half pore widths below 20 Å. SAXS suggests formation of crystalline $(HC{\equiv}C)_{0.5}$-COF material exhibiting signals at 2–3° for (001), at 4° for (110), and at 6° for (200). Furthermore, the reflections of low intensities at 7.5° for (210), at 10° for (220) were observed (Fig. S5a). The signals

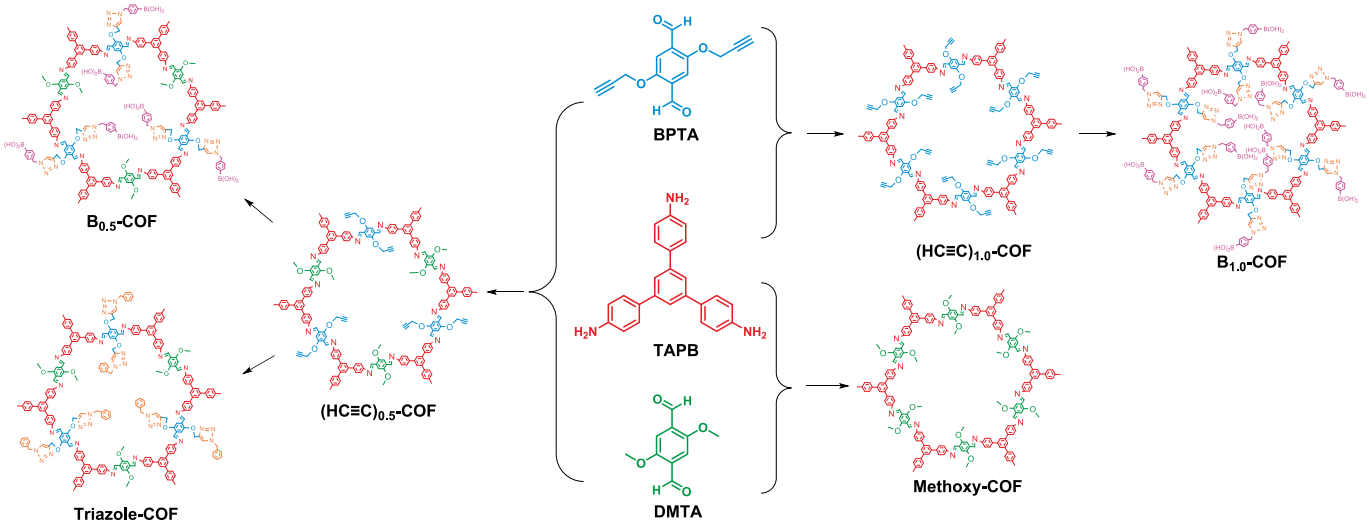

Fig. 1. An overview of the synthesized COFs based on the used monomers 2,5-bis(prop-2-yn-1-yloxy)terephthalaldehyde (BPTA), 1,3,5-tris(4-aminophenyl)benzene (TAPB), and 2,5-dimethoxyterephthalaldehyde (DMTA).

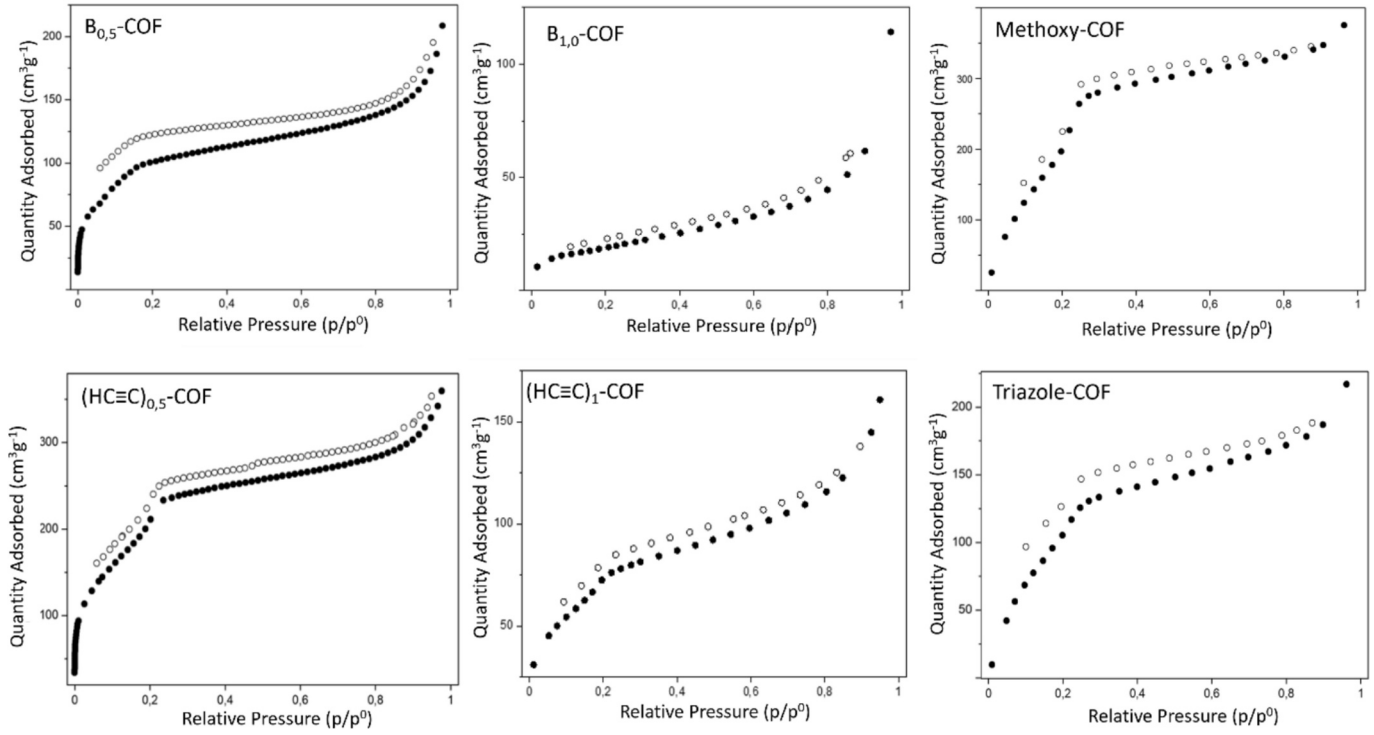

Fig. 2. Results of low-temperature N_2 physisorption over COFs: adsorption (filled symbols) and desorption (open symbols) curves.

arise from a 2D hexagonal lattice with a spacing between the centers of the hexagon repeating units of *ca.* 3.64 nm. This result is the same as previously reported distance of 36.4594 Å for TAPB-DMTA COF [54]. The intensity of the first signal enables an estimation of *ca.* 60 nm coherence length indicating the presence of *ca.* 20 units. A signal at 18 nm^{-1} suggests an interlayer spacing of *ca.* 3.5 Å, which is similar to the previously reported for TAPB-DMTA COF $c = 3.5239$ Å [54]. In general, the SAXS data suggest the crystalline structure of the synthesized materials with a hexagonal unit cell typical of two-dimensional imine-linked COFs [55–58].

The $(HC{\equiv}C)_{1.0}$-COF and $(HC{\equiv}C)_{0.5}$-COF were used for a post-synthetic functionalization to immobilize the phenylboronic acid moiety resulting in $B_{1.0}$-COF and $B_{0.5}$-COF materials, respectively. First, a click reaction was conducted, when protected with a pinacol group and possessing an azide moiety phenylboronic acid was allowed to react with the COFs bearing the propargyl groups. After this step, the band at 3300 cm^{-1} in FT-IR spectra disappeared suggesting that the materials after the click reaction possess no —C≡C—H groups (Fig. S4). Thereafter, the phenylboronic acid group was deprotected *via* a reaction with diethanol amine followed by hydrolysis in the presence of 0.1 M HCl. This step was monitored by ^{1}H NMR in solution to detect signals of the released pinacol. After functionalization, the ^{13}C MAS NMR spectra of the materials confirm the absence of signals coming from the triple bond moieties but instead exhibit a new signal at 63 ppm, which can be attested to a CH_2-group between a triazole ring and a phenylboronic acid group (Fig. 3). ^{11}B MAS NMR spectra exhibit signals in the range of 0 to

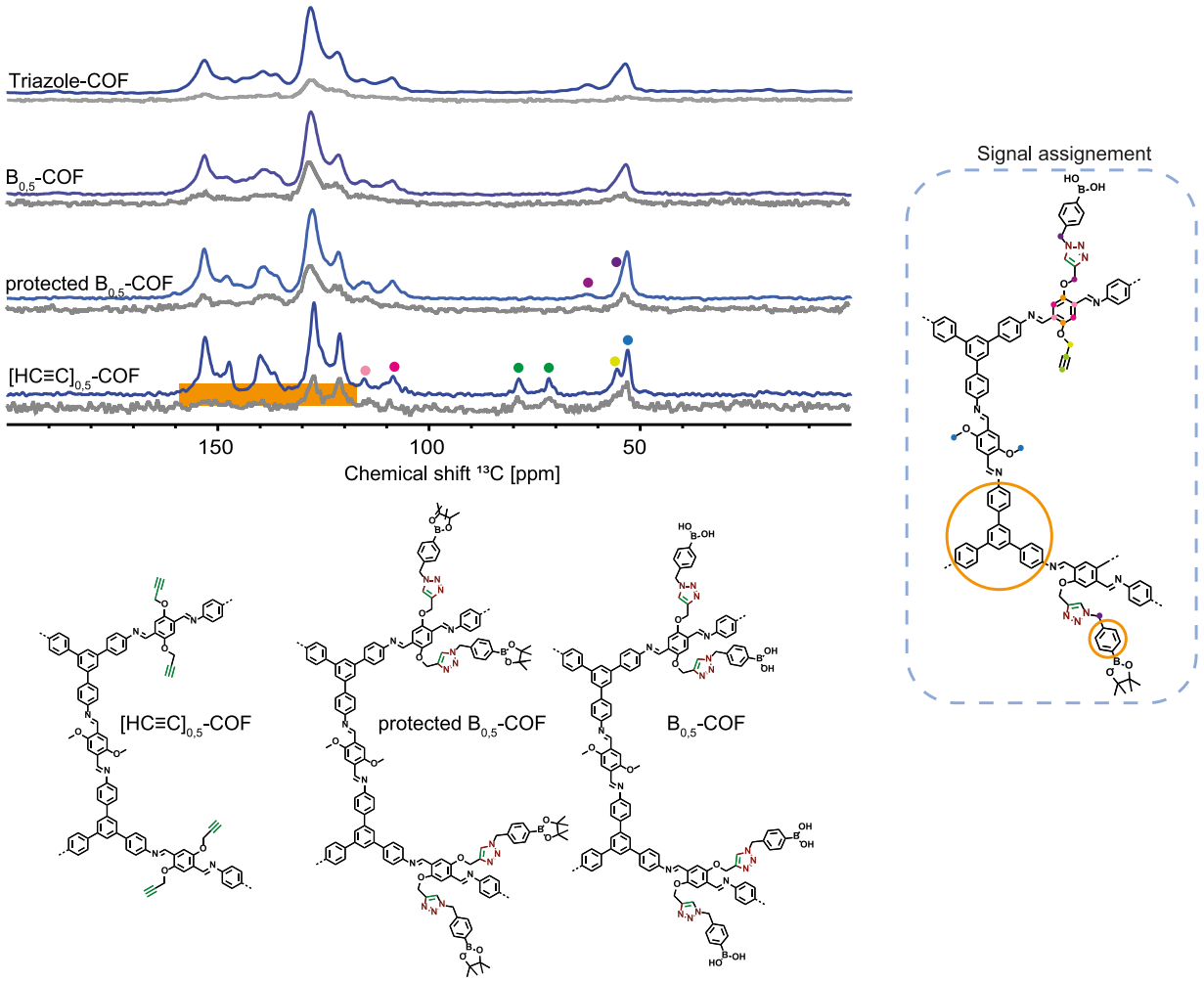

Fig. 3. ^{13}C solid-state NMR spectra of $[HC{\equiv}C]_{0.5}$-COF, as well as the protected $B_{0.5}$-COF, deprotected $B_{0.5}$-COF, and Triazole-COF.

30 ppm corresponding to boronate groups with boron in sp^2 and sp^3 hybridization (Fig. S6). $B_{0.5}$-COF and $B_{1.0}$-COF exhibit a boron content of 6.0 mg g^{-1} and 9.5 mg g^{-1}, respectively. Interestingly, the specific surface area of $B_{0.5}$-COF was 571 m^2 g^{-1}, significantly exceeding the S_{BET} of 69 m^2 g^{-1} detected for $B_{1.0}$-COF (Table S1). SEM images suggest that $B_{0.5}$-COF consists of stacked flat plates (Fig. S7). The SAXS data of $B_{0.5}$-COF exhibit the same pattern as the parent $(HC{\equiv}C)_{0.5}$-COF material suggesting the preservation of the crystalline structure during the post synthetic functionalization (Fig. S5b).

Post-synthetic functionalization of $(HC{\equiv}C)_{0.5}$-COF by a click reaction with benzyl azide was performed to yield Triazole-COF, *i.e.* a material exhibiting triazole groups and lacking phenylboronate moieties. The obtained Triazole-COF exhibited a S_{BET} of 596 m^2 g^{-1}. The SAXS pattern of Triazole-COF is similar to $B_{0.5}$-COF and $(HC{\equiv}C)_{0.5}$-COF indicating the same crystalline structure of the materials (Fig. S5c).

3.2. Sorption performance of COFs

The synthesized COFs were tested for adsorption of D-fructose. The adsorption tests were performed in carbonate buffer at pH 10, similar to the previously reported sorption over cross-linked polymers with phenylboronate groups [25]. Adsorption over hydrophobic cross-linked polymers required addition of an organic co-solvent, such as ethanol [25,28–30], whereas no organic co-solvent was necessary for adsorption over the hydrophilic COFs. As shown in Fig. 4, Methoxy-COF and $(HC{\equiv}C)_{0.5}$-COF exhibited the lowest uptakes of D-fructose, whereas loading of D-fructose over boronate-functionalized COFs was significantly higher. Interestingly, $B_{0.5}$-COF exhibited the highest D-fructose uptake despite the higher boron content in $B_{1.0}$-COF. This result can be attributed to less available space in the pores of the latter material due to a higher degree of post-synthetic functionalization, which is reflected in a dramatically lower S_{BET} of $B_{1.0}$-COF than of $B_{0.5}$-COF (Table S1). Our results corroborate with the previously reported data on pore wall functionalization of COFs: systematic increase of the functionalization degree often results in decrease of specific surface area and pore volume which frequently leads to decrease of adsorption capacity of the COFs with high degree of pore wall functionalization [59–62]. Boron content of $B_{0.5}$-COF is 6.5 mg g^{-1}, suggesting the maximal theoretical uptake of D-fructose of *ca.* 100 mg g^{-1} owing to complexation with boronate groups. Remarkably, the observed uptake of D-fructose was considerably higher, namely *ca.* 450 mg g^{-1}. We hypothesized that interactions of D-fructose with triazole rings formed upon click reaction can cause the increased loading. Testing Triazole-COF supported this hypothesis, since D-fructose loading over this material was *ca.* 280 mg g^{-1}. This loading of D-fructose is as high as over $B_{1.0}$-COF and considerably higher than over the benchmark Methoxy- and $(HC{\equiv}C)_{0.5}$-COFs.

The $B_{0.5}$-COF and Triazole-COF were tested at various pH values as Fig. 5 shows. As expected, an increase of the pH value from 5 to 10 resulted in enhanced uptake of D-fructose by $B_{0.5}$-COF. Fig. S6 summarizes the solid-state ^{11}B NMR spectra of $B_{0.5}$-COF suggesting an increased portion of the sp^3 hybridized boron after treating $B_{0.5}$-COF with a buffer at higher pH value. Since sp^3-hybidized boron favors the complexation (Fig. S1), a higher D-fructose uptake upon pH increase is expected. Interestingly, D-fructose loading over Triazole-COF also rises along with

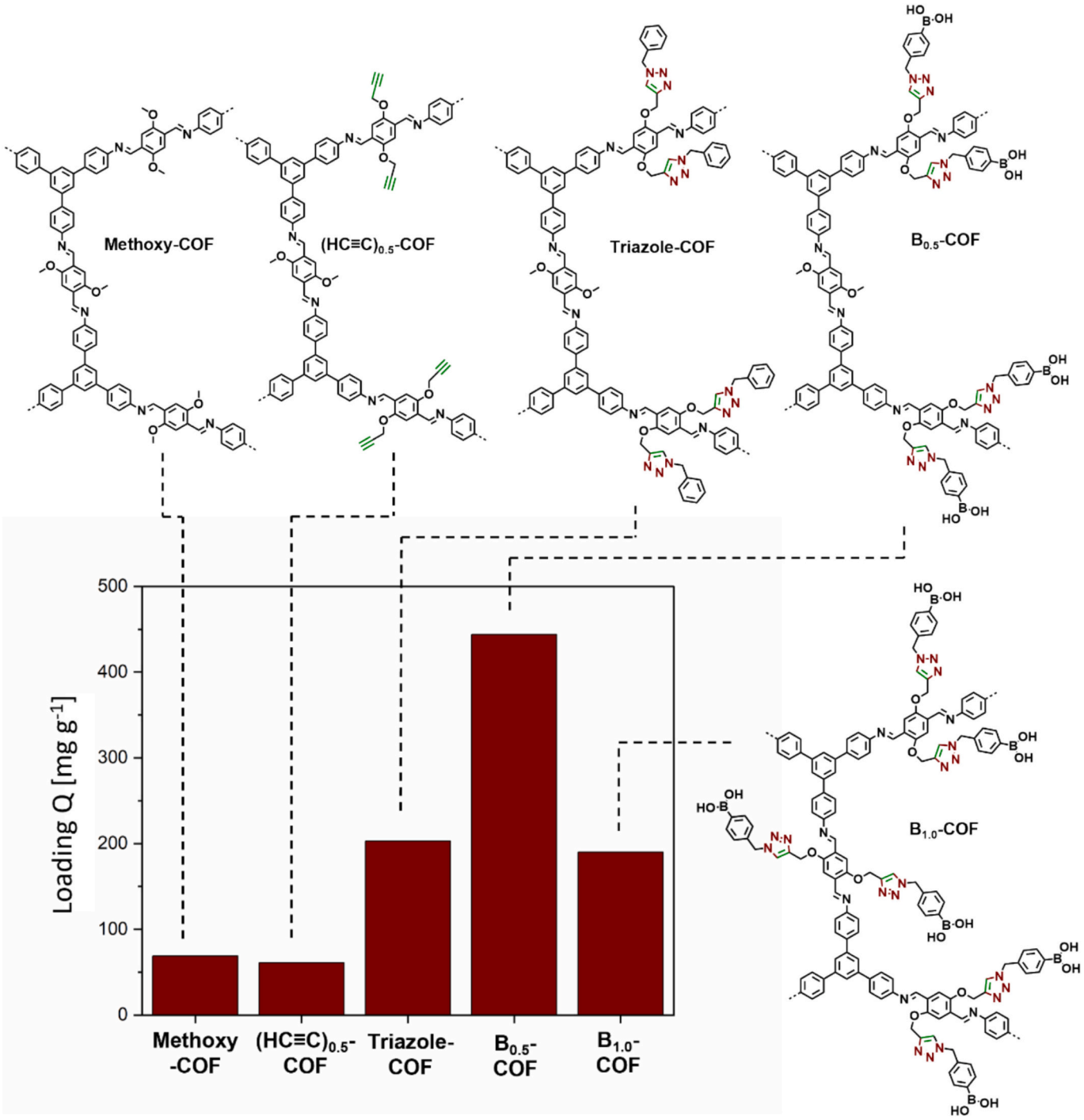

Fig. 4. Results of the adsorption tests over COFs. Adsorption conditions: 30 mg COF, 1.5 mL D-fructose (50 mg mL^{-1}) in carbonate buffer at pH 10, 3 h, 500 rpm, room temperature.

the pH increase from 5 to 10. Apparently, protonation and deprotonation of the triazole ring plays an important role in the interaction of D-fructose with the triazole moieties [63]. An increase of the pH value from 10 to 12 resulted in a significant decrease in D-fructose uptake for both $B_{0.5}$-COF and Triazole-COF, probably, owing to interactions with the materials or preferential uptake of the components of the glycine buffer by the COFs. Thus, the adsorption tests were conducted in carbonate buffer at pH 10. Time-resolved experiments suggested that the adsorption equilibrium is reached in less than 3 h and the pH value does not change during the adsorption (Fig. S8).

Next, desorption of D-fructose from $B_{0.5}$-COF was examined (Fig. 6a). Ethanol and water resulted in modest desorption efficiencies of 17 or 48 %, whereas *ca.* 72 % D-fructose was desorbed in a 1:1 water:ethanol mixture. Application of 0.5 M H_2SO_4 led to recovery of 90 % D-fructose. $B_{0.5}$-COF exhibited excellent recyclability in four adsorption-desorption cycles, as shown in Fig. 6b with minor decrease of the corrected loading and desorption efficiency from cycle to cycle. The corrected loading here refers to the total loading of D-fructose including D-fructose which was not desorbed in the previous cycles. Interestingly, protonation and deprotonation of the imine groups in the COF framework results in cyclic color changes under basic and acidic conditions as Fig. 6c shows. SAXS patterns recorded for the $B_{0.5}$-COF after adsorption of D-fructose in

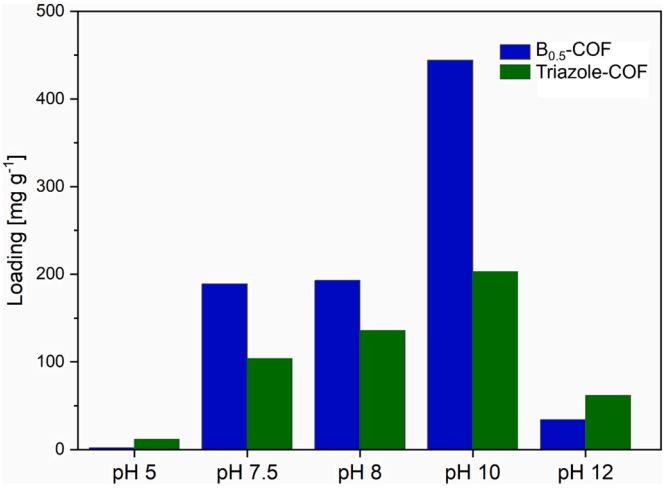

Fig. 5. Results of the adsorption tests over $B_{0.5}$-COF and Triazole-COF at different pH values. Adsorption conditions: 30 mg COF, 1.5 mL D-fructose (50 mg mL^{-1}), 3 h, 500 rpm, room temperature.

carbonate buffer at pH 10 and the desorption of D-fructose using 0.5 M H_2SO_4 indicate that the crystallinity of $B_{0.5}$-COF is preserved under these conditions (Fig. S9). Remarkably, the SAXS pattern of $B_{0.5}$-COF loaded by D-fructose exhibits an additional signal at 6.38 nm^{-1} which corresponds to the lattice constant of *ca.* 1 nm and can be tentatively attributed to the (010) of crystalline D-fructose [64]. The SAXS pattern of $B_{0.5}$-COF after desorption of D-fructose does not exhibit this peak.

Previously explored cross-linked polymers bearing phenylboronic acid groups exhibited high loading of D-fructose, but suffered from low durability of the polymer and its significant swelling during the adsorption [25]. $B_{0.5}$-COF was pelletized and soaked in a 20 % solution of D-fructose in carbonate buffer at pH 10 for 7 days at room temperature. No swelling or other changes of the pellet were observed at the end of this test suggesting an outstanding durability of $B_{0.5}$-COF under the adsorption conditions (Fig. S10a). Moreover, the SAXS analysis of the $B_{0.5}$-COF after soaking in the D-fructose solution for 7 days (Fig. S10b) suggests that the material retains crystallinity after this treatment. Analogous to the SAXS pattern of the $B_{0.5}$-COF after adsorption of D-fructose (Fig. S9a), the spectrum exhibits an additional peak at 6.38 nm^{-1} apparently coming from crystalline D-fructose [64].

Recovery of D-fructose from the glucose-fructose syrup presents the major challenge in biorefining [27]. To estimate the potential of the synthesized COFs for the separation, the adsorption isotherms for uptake of D-glucose and D-fructose by Triazole-COF and $B_{0.5}$-COF were recorded. Table 1 summarizes the parameters of the Langmuir model obtained by the fitting of the adsorption isotherms (Fig. 7). Both Triazole-COF and $B_{0.5}$-COF exhibit higher affinity for D-fructose than for D-glucose. Additionally, a maximum adsorption capacity of D-fructose is higher than of D-glucose. $B_{0.5}$-COF exhibits the maximum capacity of D-fructose of 560 mg g^{-1}. Table S2 summarizes data on previously published performance of the boron-containing adsorbents suggesting that the adsorption capacity $B_{0.5}$-COF is comparable to the best previously reported materials. Noteworthily, $B_{0.5}$-COF does not suffer from swelling and exhibits high hydrophilicity, *i.e.* can be applied using pure aqueous adsorption and desorption solutions. Fig. S11 compares hydrophilicity of $B_{0.5}$-COF with previously reported hydrophobic poly(4-vinylphenylboronic acid) cross-linked with 20 mol% of divinyl benzene [25]. Whereas the hydrophilic $B_{0.5}$-COF readily forms a suspension in water (Fig. S11a), the hydrophobic cross-linked poly(4-vinylphenylboronic acid) remains not wetted on the top of the aqueous medium (Fig. S11b).

Competitive adsorption of D-fructose and D-glucose in two solutions with the ratios of D-fructose-to-D-glucose of 1:1 and 1:4, respectively, was conducted under batch conditions. Even for a solution with high content of D-glucose, D-fructose was predominantly adsorbed over COF (Fig. 8). The separation factor in this case can be estimated as $SF = (q_{D\text{-fructose}} / q_{D\text{-glucose}}) / (c_{eq.,D\text{-fructose}} / c_{eq.,D\text{-glucose}})$, where q corresponds to the loading and $c_{eq.}$ refers to the equilibrium concentration. The separation factors are 37 and 122 for the 1:1 and 1:4 solutions, respectively,

Table 1
Adsorption capacities q_{max}, Langmuir coefficients b and coefficients of determination R^2 of the recorded isotherms *via* the Langmuir fit of the two materials after adsorption of D-fructose and D-glucose.

Entry	COF	Substrate	Adsorption capacity q_{max}	Langmuir coefficient b	Coefficient of determination R^2
1	$B_{0.5}$-COF	D-Fructose	560 mg g^{-1}	0.103	0.81
2	$B_{0.5}$-COF	D-Glucose	183 mg g^{-1}	0.038	0.91
3	Triazole-COF	D-Fructose	289 mg g^{-1}	0.071	0.86
4	Triazole-COF	D-Glucose	120 mg g^{-1}	0.038	0.72

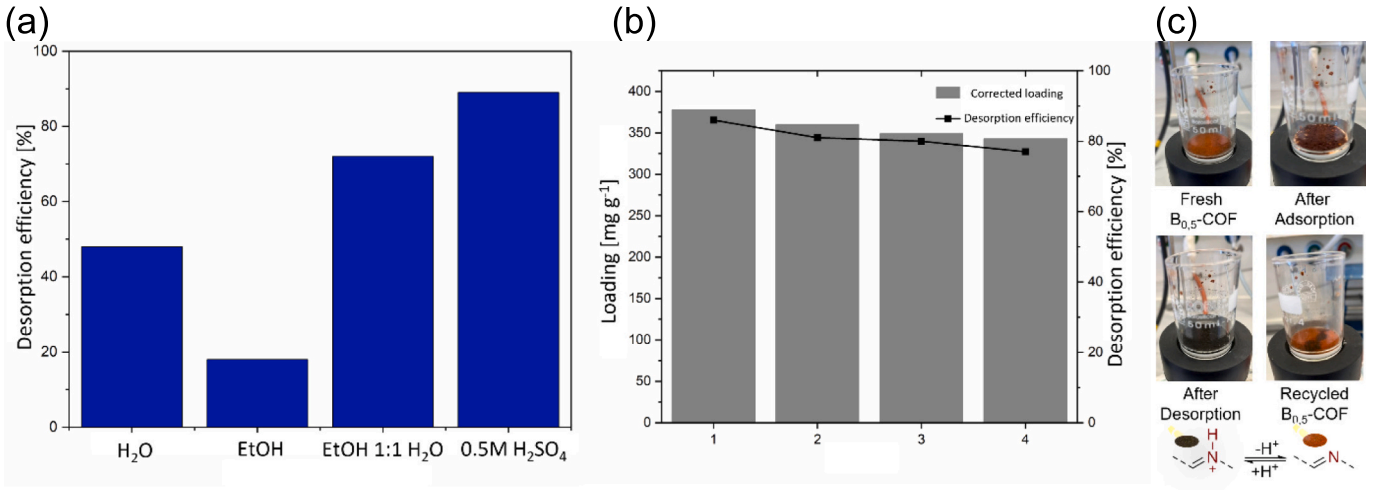

Fig. 6. (a) Results of the desorption tests over $B_{0.5}$-COF; (b) results of the recycling of $B_{0.5}$-COF, and (c) pictures of the COFs along with a scheme of protonation of an imine group in COF ring resulting in a color change. Adsorption conditions: 30 mg $B_{0.5}$-COF, 1.5 mL D-fructose (50 mg mL^{-1}), 3 h, 500 rpm, room temperature. Desorption conditions: 1.5 mL desorption solution, 3 h, 500 rpm.

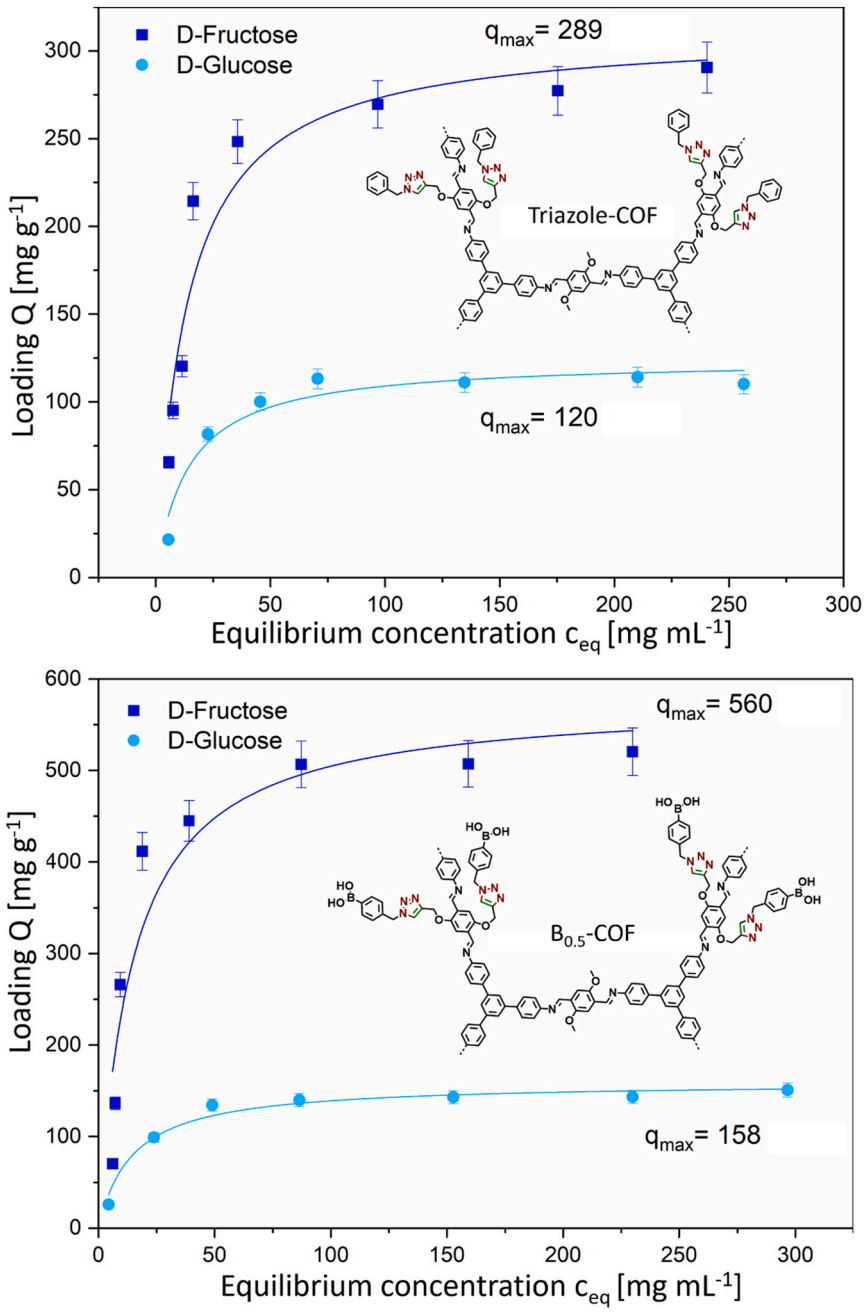

Fig. 7. Adsorption isotherms of D-fructose and D-glucose over Triazole-COF and $B_{0.5}$-COF. The experimental points were fitted using the Langmuir adsorption model. Adsorption conditions: 30 mg COF, 1.5 mL D-glucose or D-fructose, 3 h, 500 rpm, room temperature.

suggesting excellent separation and preferable adsorption of D-fructose even in a solution containing mainly D-glucose. The first results for separation of D-glucose and D-fructose over $B_{0.5}$-COF under flow conditions were also obtained. For this purpose, a 1:1 mixture of D-glucose and D-fructose in carbonate buffer at pH 10 was injected as a 10 min impulse in a column filled with $B_{0.5}$-COF. Thereafter, 0.5 M H_2SO_4 was supplied to desorb the saccharides. Fig. S12 shows the obtained mass-time diagram at which D-glucose and D-fructose were eluted as two peaks with maxima at 10 and 16 min, respectively, highlighting a great potential of the boron-functionalized COFs for separation of D-fructose and D-glucose.

Adsorption of D-fructose and D-glucose over Triazole-COF and $B_{0.5}$-COF was explored using ^{1}H, ^{13}C, and ^{11}B MAS NMR techniques. At first, Triazole-COF and $B_{0.5}$-COF were loaded with D-fructose at natural abundance and investigated by solid-state NMR (Fig. S13). The ^{1}H NMR spectra of unloaded COFs exhibit three distinct signals $\delta(^{1}H)$ at 7.5, 4.2, and 1.6 ppm corresponding to the signals of aromatic rings, methoxy groups, and aliphatic carbons, respectively. Upon D-fructose loading, the ^{1}H NMR spectra show broadened signals and the ratio between aliphatic and aromatic signals increases. Furthermore, the ^{11}B Hahn echo spectrum for $B_{0.5}$-COF changes so that the signal of ^{11}B in the sp^2 configuration is the dominant species. Although clear evidence of the D-fructose absorption could be observed, the signal intensity of the D-fructose in the ^{13}C CP spectra was insufficient and no clear assignment of the D-fructose signals was possible. Therefore, the following characterization of the specific sugar species was done with ^{13}C-1-D-glucose and ^{13}C-2-D-fructose molecules.

The ^{13}C CP (cross-polarization) and ^{13}C DE (direct excitation) MAS NMR spectra of Triazole-COF and $B_{0.5}$-COF loaded with ^{13}C-1-D-glucose and ^{13}C-2-D-fructose are shown in Fig. 9. The respective ^{1}H solid-state

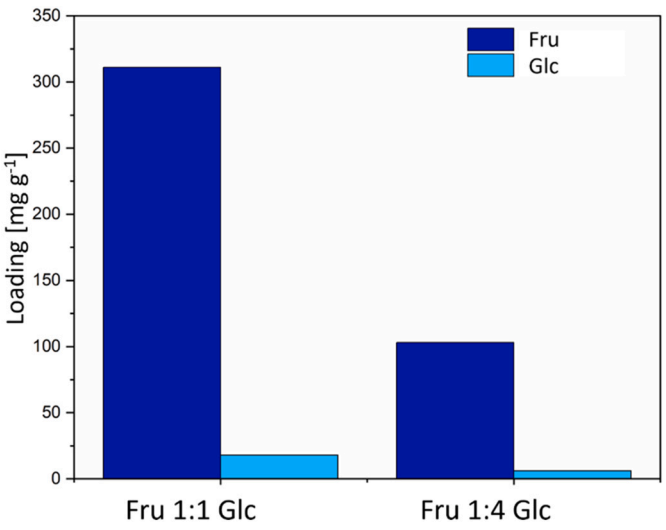

Fig. 8. Results of competitive adsorption of D-fructose (Fru) and D-glucose (Glc) with various ratios of the sugars over $B_{0.5}$-COF. Adsorption conditions: 30 mg $B_{0.5}$-COF, total concentration of D-glucose and D-fructose 50 mg mL^{-1}, 3 h, stirring at 500 rpm, room temperature.

NMR spectra (Fig. S14) show a dominant signal at 7.1 ppm (aromatic COF), two further signals at lower ppm values (methoxy group COF and sugar) as well as signals in the area from 12 to 20 ppm indicating the presence of hydrogen bonded ^{1}H environments. The signals of the aromatic building blocks of the COFs show no chemical shift changes due to adsorption of the saccharides suggesting the absence of strong interactions between adsorbates and the aromatic moieties. The aromatic signals exhibit some broadening upon adsorption indicating a less ordered structure of the loaded polymers (Fig. S13). The methoxy groups are affected by fructose loading: their resonances shift from δ(^{13}C) *ca.* 53 ppm to 55–56 ppm indicating that the methoxy groups are in proximity of the adsorbed D-glucose and D-fructose or experience a change in their chemical environment. The intensity of the signals in the ^{13}C DE NMR spectra provides an estimate of the mobility of the species since more intense signals result from more mobile moieties. Fig. 9 shows that saccharides adsorbed over Triazole-COF exhibit a significantly higher mobility (higher signal intensity in the ^{13}C DE NMR spectra) than ^{13}C-1-D-glucose and ^{13}C-2-D-fructose adsorbed over $B_{0.5}$-COF, apparently, owing to formation of covalent bonding between the saccharides and the boronate groups of the $B_{0.5}$-COF and less rigid non-covalent interactions between the saccharides and the triazole functionalities. Table 2 shows distributions of the forms of the adsorbates obtained *via* integration of the corresponding resonances of C1 for ^{13}C-1-D-glucose and C2 for ^{13}C-2-

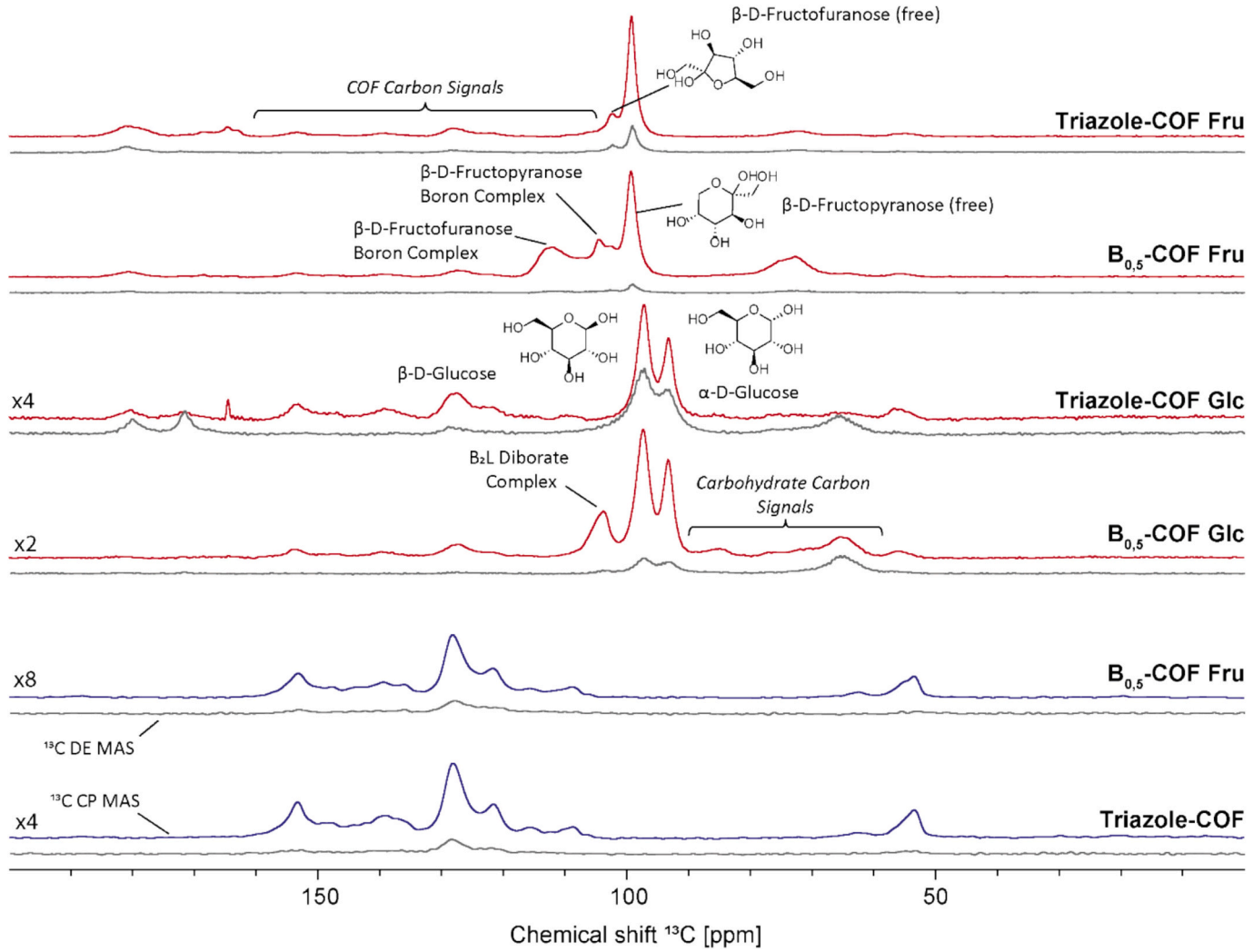

Fig. 9. ^{13}C CP and ^{13}C DE MAS NMR spectra of Triazole-COF and $B_{0.5}$-COF loaded with ^{13}C-2-D-fructose (Fru) or ^{13}C-1-D-glucose (Glc). All spectra are scaled on the number of scans. In each case, the upper spectrum is the ^{13}C CP MAS spectrum (d1 = 2 s) and the lower is the ^{13}C DE spectrum measured with a recycle delay of 2 s with assigned signals.

Table 2
Assignments of the signals of the labeled atoms observed in ^{13}C MAS NMR spectra of the adsorbed ^{13}C-1-D-glucose and ^{13}C-2-D-fructose over Triazole-COF and $B_{0.5}$-COF. Percentages of the forms of the saccharides calculated upon deconvolution of the spectra are provided in parentheses.

Entry	COF	Saccharide	Free saccharide						Complexed saccharide	
			Open-chain form	Unknown	α-Pyranose	β-Pyranose	α-Furanose	β-Furanose	Bi-and tridental complex monoborate	B_2L diborate complexes
1	Triazole-COF	^{13}C-1-D-glucose	180.5 ppm (8 %)	171.5 ppm (8 %)	93.2 ppm (24 %)	97.1 ppm (60 %)	–	–	–	–
2	$B_{0.5}$-COF	^{13}C-1-D-glucose	–	–	93.2 ppm (28 %)	97.3 ppm (49 %)	–	–	–	104.3 ppm (23 %)
3	Triazole-COF	^{13}C-2-D-fructose	181.3 ppm (16 %)	178.9 ppm (10 %) 171.4 ppm (3 %) 165.2 ppm (3 %)	99.7 ppm (8 %)	99.1 ppm (43 %)	104.8 ppm (9 %)	102.4 ppm (10 %)	–	–
4	$B_{0.5}$-COF	^{13}C-2-D-fructose	181.1 ppm (10 %)	171.2 ppm (2 %)	–	99.2 ppm (38 %)	104.5 ppm (9 %)	102.6 ppm (8 %)	111.7 ppm (34 %)	–

D-fructose of ^{13}C DE spectra with a long interscan delay of 20 s (Fig. S15). Fig. S16 shows the overlay of ^{13}C DE spectra of d1 = 2 s and d1 = 20 s, for which only very small changes in the relative signal intensities are observed supporting the quantitative character of the analyses. Table 2 summarizes the assignment of the signals made based on literature data [25,65–69]. Interestingly, most of the adsorbed D-glucose and D-fructose are present as free saccharides, whereas the percentages of the complexed saccharides were estimated to be 23 % for D-glucose and 34 % for D-fructose. Formation of bi- and/or tridental monoborate complexes of D-fructose was observed, whereas D-glucose forms a diborate complex upon adsorption. Signals of the labeled saccharides in the range of carbonyl moieties from 165 to 180 ppm were observed in the spectra of the loaded samples (Table 2 and Fig. S15). Contributions of these species for Triazole-COF are significantly higher than for $B_{0.5}$-COF. The most intensive signal at 180 ppm can be tentatively assigned to an open-chain form of a saccharide – though normally the contribution of the open-chain substrate does not exceed a few percent. The reasons for the signals at 165 to 178 ppm remain unknown – apparently, they are caused by the species resulting from interactions of the substrates with the COFs. The percentage of the unknown products for the adsorption of saccharides on $B_{0.5}$-COF is low, and its evolution upon adsorption-desorption cycles will be explored in detail in the future studies.

^{11}B MAS NMR spectra of the loaded $B_{0.5}$-COF exhibit narrow signals at 11.7, 8.0, and 7.2 ppm for D-glucose and 11.7 and 7.5 ppm for D-fructose, respectively, suggesting well-defined environments of the sp^3-hybridized boron. Interestingly, a resonance at 25.0 ppm corresponding to sp^2-hybridized boron was also observed in the spectrum of $B_{0.5}$-COF loaded with D-glucose (Fig. S17). To summarize, the MAS NMR study revealed covalent complexation of the adsorbates with the boronate groups and non-covalent interactions with the other moieties of the polymers manifested in less mobile saccharide molecules in $B_{0.5}$-COF and more mobile adsorbates in Triazole-COF.

4. Conclusion

In this work, two-dimensional COFs with propargyl appending groups were synthesized and post-synthetically modified by azide click reaction to obtain materials with boronate functionalities. The prepared COFs exhibit remarkable sorption properties, such as high D-fructose sorption capacity (Langmuir maximum capacity is 560 mg g^{-1}), high selectivity for D-fructose adsorption from its mixture with D-glucose, recyclability, no swelling upon adsorption, and hydrophilicity. Apparently, both boronate moieties and triazole rings are of importance for the uptake of the saccharides. Overall, this work demonstrates an outstanding potential of the boronate- and triazole COFs as adsorbents for efficient separation of D-glucose and D-fructose.

CRediT authorship contribution statement

Tobias Riedl: Writing – review & editing, Writing – original draft, Supervision, Methodology, Investigation, Formal analysis, Conceptualization. **Pia Groß:** Writing – review & editing, Investigation. **Leonie Sophie Häser:** Investigation. **Runa Tschekorsky Orloff:** Writing – review & editing, Investigation. **Theresa Röper:** Writing – review & editing, Investigation. **Thomas Fuchs:** Writing – review & editing, Investigation. **Stephanie Bachmann:** Writing – review & editing, Methodology, Investigation. **Ann-Christin Pöppler:** Writing – review & editing, Writing – original draft, Supervision, Investigation. **Herwig Peterlik:** Writing – review & editing, Investigation. **Andreas Jupke:** Writing – review & editing, Investigation. **Regina Palkovits:** Writing – review & editing, Resources. **Irina Delidovich:** Writing – review & editing, Writing – original draft, Supervision, Project administration, Investigation, Conceptualization.

Declaration of competing interest

The authors declare that they have no known competing financial interests or personal relationships that could have appeared to influence the work reported in this paper.

Acknowledgements

We would like to thank Noah Avraham-Radermacher and Heike Bergstein from the RWTH Aachen University for carrying out the HPLC, N_2 physisorption, and ICP-OES measurements. We thank Valérie Toussaint from the TU Wien for providing us with a photo of poly(4-vinylphenylboronic acid) cross-linked with 20 mol% of divinyl benzene. This work was funded by Cluster of Excellence Fuel Science Center (EXC 2186, ID: 390919832) funded by the Excellence Initiative by the German federal and state governments to promote science and research at German Universities. The authors acknowledge TU Wien Bibliothek for financial support through its Open Access Funding Programme.

Appendix A. Supplementary data

Supplementary data to this article can be found online at https://doi.

org/10.1016/j.cej.2025.168357.

Data availability

Data will be made available on request.

References

[1] J. Popp, Z. Lakner, M. Harangi-Rákos, M. Fári, The effect of bioenergy expansion: food, energy, and environment, Renew. Sust. Energ. Rev. 32 (2014) 559–578, https://doi.org/10.1016/j.rser.2014.01.056.

[2] G.W. Huber, S. Iborra, A. Corma, Synthesis of transportation fuels from biomass: chemistry, catalysts, and engineering, Chem. Rev. 106 (2006) 4044–4098, https://doi.org/10.1021/cr068360d.

[3] J.N. Chheda, G.W. Huber, J.A. Dumesic, Liquid-phase catalytic processing of biomass-derived oxygenated hydrocarbons to fuels and chemicals, Angew. Chem. Int. Ed. 46 (2007) 7164–7183, https://doi.org/10.1002/anie.200604274.

[4] R. Rinaldi, F. Schuth, Design of solid catalysts for the conversion of biomass, Energy Environ. Sci. 2 (2009) 610–626, https://doi.org/10.1039/B902668A.

[5] J.J. Bozell, G.R. Petersen, Technology development for the production of biobased products from biorefinery carbohydrates-the US Department of Energy's "Top 10" revisited, Green Chem. 12 (2010) 539–554, https://doi.org/10.1039/b922014c.

[6] P. Gallezot, Conversion of biomass to selected chemical products, Chem. Soc. Rev. 41 (2012) 1538–1558, https://doi.org/10.1039/C1CS15147A.

[7] M. Yabushita, H. Kobayashi, A. Fukuoka, Catalytic transformation of cellulose into platform chemicals, Appl. Catal. B Environ. 145 (2014) 1–9, https://doi.org/10.1016/j.apcatb.2013.01.052.

[8] I. Delidovich, P.J.C. Hausoul, L. Deng, R. Pfützenreuter, M. Rose, R. Palkovits, Alternative monomers based on lignocellulose and their use for polymer production, Chem. Rev. 116 (2016) 1540–1599, https://doi.org/10.1021/acs.chemrev.5b00354.

[9] J. Artz, R. Palkovits, Chemical building blocks from carbohydrates, Curr. Opin. Green Sustain. Chem. 14 (2018) 14–18, https://doi.org/10.1016/j.cogsc.2018.05.005.

[10] L.T. Mika, E. Cséfalvay, Á. Németh, Catalytic conversion of carbohydrates to initial platform chemicals: chemistry and sustainability, Chem. Rev. 118 (2018) 505–613, https://doi.org/10.1021/acs.chemrev.7b00395.

[11] A. Jaswal, P.P. Singh, T. Mondal, Furfural – a versatile, biomass-derived platform chemical for the production of renewable chemicals, Green Chem. 24 (2022) 510–551, https://doi.org/10.1039/D1GC03278J.

[12] L. Goswami, R. Kayalvizhi, P.K. Dikshit, K.C. Sherpa, S. Roy, A. Kushwaha, B. S. Kim, R. Banerjee, S. Jacob, R.C. Rajak, A critical review on prospects of bio-refinery products from second and third generation biomasses, Chem. Eng. J. 448 (2022) 137677, https://doi.org/10.1016/j.cej.2022.137677.

[13] T. Werpy, G. Petersen, Top value added chemicals from biomass: volume I–results of screening for potential candidates from sugars and synthesis gas, in: National Renewable Energy Lab.(NREL), Golden, CO (United States), 2004. https://www.nrel.gov/docs/fy04osti/35523.pdf.

[14] A.A. Rosatella, S.P. Simeonov, R.F.M. Frade, C.A.M. Afonso, 5-Hydroxymethylfurfural (HMF) as a building block platform: biological properties, synthesis and synthetic applications, Green Chem. 13 (2011) 754–793, https://doi.org/10.1039/C0GC00401D.

[15] E. de Jong, H.A. Visser, A.S. Dias, C. Harvey, G.-J.M. Gruter, The road to bring FDCA and PEF to the market, Polymers 14 (2022) 943, https://doi.org/10.3390/polym14050943.

[16] R.-J. van Putten, J.C. van der Waal, M. Harmse, H.H. van de Bovenkamp, E. de Jong, H.J. Heeres, A comparative study on the reactivity of various ketohexoses to furanics in methanol, ChemSusChem 9 (2016) 1827–1834, https://doi.org/10.1002/cssc.201600252.

[17] S. Wu, R. Snajdrova, J.C. Moore, K. Baldenius, U.T. Bornscheuer, Biocatalysis: enzymatic synthesis for industrial applications, Angew. Chem. Int. Ed. 60 (2021) 88–119, https://doi.org/10.1002/anie.202006648.

[18] L.M. Hanover, J.S. White, Manufacturing, composition, and applications of fructose, Am. J. Clin. Nutr. 58 (1993) 724S–732S, https://doi.org/10.1093/ajcn/58.5.724S.

[19] H.J. Bieser, A.J. De Rosset, Continuous countercurrent separation of saccharides with inorganic adsorbents, Starch - Stärke 29 (1977) 392–397, https://doi.org/10.1002/star.19770291108.

[20] S.J. Angyal, G.S. Bethell, R.J. Beveridge, The separation of sugars and of polyols on cation-exchange resins in the calcium form, Carbohydr. Res. 73 (1979) 9–18, https://doi.org/10.1016/S0008-6215(00)85471-3.

[21] Y.A. Beste, M. Lisso, G. Wozny, W. Arlt, Optimization of simulated moving bed plants with low efficient stationary phases: separation of fructose and glucose, J. Chromatogr. A 868 (2000) 169–188, https://doi.org/10.1016/S0021-9673(99)01136-X.

[22] D.A. Luz, A.K.O. Rodrigues, F.R.C. Silva, A.E.B. Torres, C.L. Cavalcante, E.S. Brito, D.C.S. Azevedo, Adsorptive separation of fructose and glucose from an agroindustrial waste of cashew industry, Bioresour. Technol. 99 (2008) 2455–2465, https://doi.org/10.1016/j.biortech.2007.04.063.

[23] S.A. Barker, B.W. Hatt, P.J. Somers, R.R. Woodbury, The use of poly(4-vinylbenzeneboronic acid) resins in the fractionation and interconversion of carbohydrates, Carbohydr. Res. 26 (1973) 55–64, https://doi.org/10.1016/S0008-6215(00)85021-1.

[24] M. Glad, S. Ohlson, L. Hansson, M.-O. Mánsson, K. Mosbach, High-performance liquid affinity chromatography of nucleosides, nucleotides and carbohydrates with boronic acid-substituted microparticulate silica, J. Chromatogr. A 200 (1980) 254–260, https://doi.org/10.1016/S0021-9673(00)84944-4.

[25] G. Schroer, J. Deischter, T. Zensen, J. Kraus, A.-C. Pöppler, L. Qi, S. Scott, I. Delidovich, Structure-performance correlations of cross-linked boronic acid polymers as adsorbents for recovery of fructose from glucose–fructose mixtures, Green Chem. 22 (2020) 550–562, https://doi.org/10.1039/C9GC03151K.

[26] K. Reske, H. Schott, Column-chromatographic separation of neutral sugars on a dihydroxyboryl-substituted polymer, Angew. Chem. Int. Ed. 12 (1973) 417–418, https://doi.org/10.1002/anie.197304171.

[27] I. Delidovich, V. Toussaint, Adsorptive separation of saccharides and polyols over materials functionalized with boronate groups, Green Chem. 26 (2024) 720–738, https://doi.org/10.1039/D3GC04049F.

[28] G. Schroer, V. Toussaint, S. Bachmann, A.-C. Pöppler, C.H. Gierlich, I. Delidovich, Functional phenylboronate polymers for the recovery of diols, sugar alcohols, and saccharides from aqueous solution, ChemSusChem 14 (2021) 5207–5215, https://doi.org/10.1002/cssc.202002887.

[29] G. Schroer, V. Toussaint, B. Heyman, J. Büchs, A.-C. Pöppler, I. Delidovich, Recovery of biobased 2,3-butanediol from fermentation broths by liquid-phase adsorption onto phenylboronate polymers, Curr. Res. Green Sustain. Chem. 5 (2022) 100297, https://doi.org/10.1016/j.crgsc.2022.100297.

[30] L.V. Daza-Serna, V. Toussaint, A.R. Mach-Aigner, R.L. Mach, P. Kessler, S. Bachmann, A.-C. Pöppler, A. Friedl, I. Delidovich, Assessment of the recovery of erythritol using boronic acid polymers, Ind. Eng. Chem. Res. 63 (2024) 20677–20687, https://doi.org/10.1021/acs.iecr.4c01224.

[31] Z. Wang, M. Wang, X. Lyu, C. Wang, Y. Tong, X. Hua, R. Yang, Recycling preparation of high-purity tagatose from galactose using one-pot boronate affinity adsorbent-based adsorption-assisted isomerization and simultaneous purification, Chem. Eng. J. 446 (2022) 137089, https://doi.org/10.1016/j.cej.2022.137089.

[32] M. Wang, L. Wang, X. Hua, R. Yang, Production of high-purity lactulose via an integrated one-pot boronate affinity adsorbent based adsorption-assisted isomerization and simultaneous purification, Food Chem. 429 (2023) 136935, https://doi.org/10.1016/j.foodchem.2023.136935.

[33] X. Zhu, M. Wang, X. Hua, C. Yao, R. Yang, An innovative and sustainable adsorption-assisted isomerization strategy for the production and simultaneous purification of high-purity lactulose from lactose isomerization, Chem. Eng. J. 406 (2021) 126751, https://doi.org/10.1016/j.cej.2020.126751.

[34] M. Wang, F. Ye, H. Wang, H. Admassu, M.A.A. Gasmalla, X. Hua, R. Yang, High efficiency selective and reversible capture of lactulose using new boronic acid-functionalized porous polymeric monoliths, Chem. Eng. J. 370 (2019) 1274–1285, https://doi.org/10.1016/j.cej.2019.03.264.

[35] Q. Meng, M. Rong, H. Xing, J. Yu, Y. Wang, X. Wei, R.-A. Chi, C. Chen, H. Liu, L. Yang, One-step synthesis of boronic acid-functionalized hypercrosslinked polymers for efficient separation of 1,2,4-butanetriol, Sep. Purif. Technol. 314 (2023) 123436, https://doi.org/10.1016/j.seppur.2023.123436.

[36] G. Wang, W. He, L. Wang, X. Lyu, M. Wang, R. Yang, Development of boronate affinity adsorbent bearing -B(OH)2 and F groups with low pKa value for enhanced production and purification of lactulose through adsorption-assisted bio-isomerization of lactose, Food Chem. 479 (2025) 143779, https://doi.org/10.1016/j.foodchem.2025.143779.

[37] G. Wang, W. He, Y. Sun, Y. Lu, M. Wang, R. Yang, Boronate affinity adsorbent-mediated isomerization of monosaccharides and disaccharides: affinity-driven divergence and adsorption strategy optimization, Chem. Eng. J. (2025) 165763, https://doi.org/10.1016/j.cej.2025.165763.

[38] H.L. Weith, J.L. Wiebers, P.T. Gilham, Synthesis of cellulose derivatives containing the dihydroxyboryl group and a study of their capacity to form specific complexes with sugars and nucleic acid components, Biochemistry 9 (1970) 4396–4401, https://doi.org/10.1021/bi00824a021.

[39] J.C. Dore, P.C. Wankat, Multicomponent cycling zone adsorption, Chem. Eng. Sci. 31 (1976) 921–927, https://doi.org/10.1016/0009-2509(76)87042-X.

[40] M. Wang, F. Ye, H. Wang, H. Admassu, Y. Feng, X. Hua, R. Yang, Phenylboronic acid functionalized adsorbents for selective and reversible adsorption of lactulose from syrup mixtures, J. Agric. Food Chem. 66 (2018) 9269–9281, https://doi.org/10.1021/acs.jafc.8b02152.

[41] S. Mohapatra, N. Panda, P. Pramanik, Boronic acid functionalized superparamagnetic iron oxide nanoparticle as a novel tool for adsorption of sugar, Mater. Sci. Eng. C 29 (2009) 2254–2260, https://doi.org/10.1016/j.msec.2009.05.017.

[42] L. Gu, Y. Wang, J. Han, L. Wang, X. Tang, C. Li, L. Ni, Phenylboronic acid-functionalized core–shell magnetic composite nanoparticles as a novel protocol for selective enrichment of fructose from a fructose–glucose aqueous solution, New J. Chem. 41 (2017) 13399–13407, https://doi.org/10.1039/C7NJ02106B.

[43] Y.-H. Zhao, D.F. Shantz, Phenylboronic acid functionalized SBA-15 for sugar capture, Langmuir 27 (2011) 14554–14562, https://doi.org/10.1021/la203121u.

[44] D. Li, Y. Chen, Z. Liu, Boronate affinity materials for separation and molecular recognition: structure, properties and applications, Chem. Soc. Rev. 44 (2015) 8097–8123, https://doi.org/10.1039/C5CS00013K.

[45] A.P. Côté, A.I. Benin, N.W. Ockwig, M. Keeffe, A.J. Matzger, O.M. Yaghi, Porous, crystalline, covalent organic frameworks, Science 310 (2005) 1166, https://doi.org/10.1126/science.1120411.

[46] Z. Wang, S. Zhang, Y. Chen, Z. Zhang, S. Ma, Covalent organic frameworks for separation applications, Chem. Soc. Rev. 49 (2020) 708–735, https://doi.org/10.1039/C9CS00827F.

[47] C. Gao, J. Bai, Y. He, Q. Zheng, W. Ma, Z. Lin, Post-synthetic modification of phenylboronic acid-functionalized magnetic covalent organic frameworks for

specific enrichment of N-linked glycopeptides, ACS Sustain. Chem. Eng. 7 (2019) 18926–18934, https://doi.org/10.1021/acssuschemeng.9b04293.
[48] Y. Wu, N. Sun, C. Deng, Construction of magnetic covalent organic frameworks with inherent hydrophilicity for efficiently enriching endogenous glycopeptides in human saliva, ACS Appl. Mater. Interfaces 12 (2020) 9814–9823, https://doi.org/10.1021/acsami.9b22601.
[49] Y. Wang, S. Wu, D. Wu, J. Shen, Y. Wei, C. Wang, Amino bearing core-shell structured magnetic covalent organic framework nanospheres: preparation, postsynthetic modification with phenylboronic acid and enrichment of monoamine neurotransmitters in human urine, Anal. Chim. Acta 1093 (2020) 61–74, https://doi.org/10.1016/j.aca.2019.09.078.
[50] Z. Chang, Y. Liang, S. Wang, L. Qiu, Y. Lu, L. Feng, Z. Sui, Q. Chen, A novel fluorescent covalent organic framework containing boric acid groups for selective capture and sensing of cis-diol molecules, Nanoscale 12 (2020) 23748–23755, https://doi.org/10.1039/D0NR06110G.
[51] Z. Wang, T. Zou, S. Feng, F. Wu, J. Zhang, Boronic acid-functionalized magnetic porphyrin-based covalent organic framework for selective enrichment of cis-diol-containing nucleosides, Anal. Chim. Acta 1278 (2023) 341691, https://doi.org/10.1016/j.aca.2023.341691.
[52] Q. Zhang, F. Luo, Fabricating boron-functionalized covalent organic framework with remarkable potential in handling cationic, anionic, and gaseous nuclear wastes, Adv. Funct. Mater. 34 (2024) 2401775, https://doi.org/10.1002/adfm.202401775.
[53] R.K. Harris, E.D. Becker, R. Goodfellow, P. Granger, NMR nomenclature nuclear spin properties and conventions for chemical shifts, Pure Appl. Chem. 73 (2001) 1795–1818, https://doi.org/10.1351/pac200173111795.
[54] H. Xu, J. Gao, D. Jiang, Stable, crystalline, porous, covalent organic frameworks as a platform for chiral organocatalysts, Nat. Chem. 7 (2015) 905–912, https://doi.org/10.1038/nchem.2352.
[55] P.J. Waller, Y.S. AlFaraj, C.S. Diercks, N.N. Jarenwattananon, O.M. Yaghi, Conversion of imine to oxazole and thiazole linkages in covalent organic frameworks, J. Am. Chem. Soc. 140 (2018) 9099–9103, https://doi.org/10.1021/jacs.8b05830.
[56] P. Albacete, J.I. Martínez, X. Li, A. López-Moreno, S.a. Mena-Hernando, A. E. Platero-Prats, C. Montoro, K.P. Loh, E.M. Pérez, F. Zamora, Layer-stacking-driven fluorescence in a two-dimensional imine-linked covalent organic framework, J. Am. Chem. Soc. 140 (2018) 12922–12929, https://doi.org/10.1021/jacs.8b07450.
[57] Y. Li, L. Guo, Y. Lv, Z. Zhao, Y. Ma, W. Chen, G. Xing, D. Jiang, L. Chen, Polymorphism of 2D imine covalent organic frameworks, Angew. Chem. Int. Ed. 60 (2021) 5363–5369, https://doi.org/10.1002/anie.202015130.
[58] F. Haase, E. Troschke, G. Savasci, T. Banerjee, V. Duppel, S. Dörfler, M.M. J. Grundei, A.M. Burow, C. Ochsenfeld, S. Kaskel, B.V. Lotsch, Topochemical conversion of an imine- into a thiazole-linked covalent organic framework enabling real structure analysis, Nat. Commun. 9 (2018) 2600, https://doi.org/10.1038/s41467-018-04979-y.
[59] A. Nagai, Z. Guo, X. Feng, S. Jin, X. Chen, X. Ding, D. Jiang, Pore surface engineering in covalent organic frameworks, Nat. Commun. 2 (2011) 536, https://doi.org/10.1038/ncomms1542.
[60] W. Ji, L. Xiao, Y. Ling, C. Ching, M. Matsumoto, R.P. Bisbey, D.E. Helbling, W. R. Dichtel, Removal of GenX and perfluorinated alkyl substances from water by amine-functionalized covalent organic frameworks, J. Am. Chem. Soc. 140 (2018) 12677–12681, https://doi.org/10.1021/jacs.8b06958.
[61] N. Huang, R. Krishna, D. Jiang, Tailor-made pore surface engineering in covalent organic frameworks: systematic functionalization for performance screening, J. Am. Chem. Soc. 137 (2015) 7079–7082, https://doi.org/10.1021/jacs.5b04300.
[62] Y. Xie, T. Pan, Q. Lei, C. Chen, X. Dong, Y. Yuan, J. Shen, Y. Cai, C. Zhou, I. Pinnau, Y. Han, Ionic functionalization of multivariate covalent organic frameworks to achieve an exceptionally high iodine-capture capacity, Angew. Chem. Int. Ed. 60 (2021) 22432–22440, https://doi.org/10.1002/anie.202108522.
[63] L.D. Hansen, B.D. West, E.J. Baca, C.L. Blank, Thermodynamics of proton ionization from some substituted 1,2,3-triazoles in dilute aqueous solution, J. Am. Chem. Soc. 90 (1968) 6588–6592, https://doi.org/10.1021/ja01026a003.
[64] X. Yao, C. Fu, S. Zhang, L. Cheng, Z. Jiang, Structure investigation of β-D-fructose crystal under high pressure: Raman scattering, IR absorption, and synchrotron X-ray diffraction, J. Mol. Struct. 1220 (2020) 128746, https://doi.org/10.1016/j.molstruc.2020.128746.
[65] J.C. Norrild, H. Eggert, Evidence for mono- and bisdentate boronate complexes of glucose in the furanose form. application of 1JC-C coupling constants as a structural probe, J. Am. Chem. Soc. 117 (1995) 1479–1484, https://doi.org/10.1021/ja00110a003.
[66] R. Smoum, A. Rubinstein, M. Srebnik, Combined 1H, 13C and 11B NMR and mass spectral assignments of boronate complexes of D-(+)-glucose, D-(+)-mannose, methyl-α-D-glucopyranoside, methyl-β-D-galactopyranoside and methyl-α-D-mannopyranoside, Magn. Reson. Chem. 41 (2003) 1015–1020, https://doi.org/10.1002/mrc.1301.
[67] R. van den Berg, J.A. Peters, H. van Bekkum, The structure and (local) stability constants of borate esters of mono- and di-saccharides as studied by 11B and 13C NMR spectroscopy, Carbohydr. Res. 253 (1994) 1–12, https://doi.org/10.1016/0008-6215(94)80050-2.
[68] J.C. Norrild, H. Eggert, Boronic acids as fructose sensors. Structure determination of the complexes involved using 1JCC coupling constants, J. Chem. Soc. Perkin Trans. 2 (1996) 2583–2588, https://doi.org/10.1039/p29960002583.
[69] S.P. Draffin, P.J. Duggan, S.A.M. Duggan, J.C. Norrild, Highly selective lipophilic diboronic acid that transports fructose as the trisdentate 2,3,6-β-d-fructofuranose ester, Tetrahedron 59 (2003) 9075–9082, https://doi.org/10.1016/j.tet.2003.09.068.